

THERMALLY DISTINCT CRATERS NEAR HRAD VALLIS, MARS. A. R. Morris¹ and P. J. Mouginis-Mark¹, ¹Hawai'i Institute of Geophysics and Planetology, 1680 East-West Rd, POST 504, Honolulu, HI 96822.

Introduction: The terrain surrounding Hrad Vallis, NW Elysium Planitia at 34°N, 218°W, is geologically distinct from the surrounding landscape. The area is characterized by unusual flow-like deposits and channel systems that extend radially from the slopes of Elysium Mons [1] (Fig. 1). Various formation mechanisms have been proposed for Hrad Vallis using Viking Orbiter [1] and Mars Orbiter Camera (MOC) images [2]. Previous workers noted the presence of depressions within the flow deposit that appear to have been formed by processes other than impact cratering [2-4]. Presently, no rigorous models exist to explain the formation of these distinct craters. The primary goal of the current study is to assess possible formation mechanisms for the craters by way of a geomorphologic and topographic examination utilizing a variety of data available.

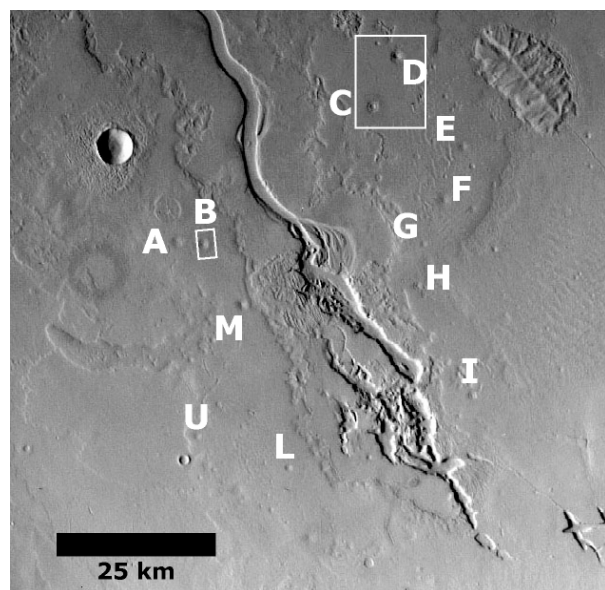


Figure 1. Viking mosaic of Hrad Vallis region. Thermally distinct craters identified by letters. White boxes indicate location of subsequent figures. Viking images 541A10-

High-resolution MOLA-derived topography and MOC images, Thermal Emission Infrared Imaging Spectrometer visible wavelength (THEMIS VIS), and day and night THEMIS infrared (THEMIS IR) image data provide insight into the topographic, morphologic and thermal properties of craters in the Hrad Vallis region.

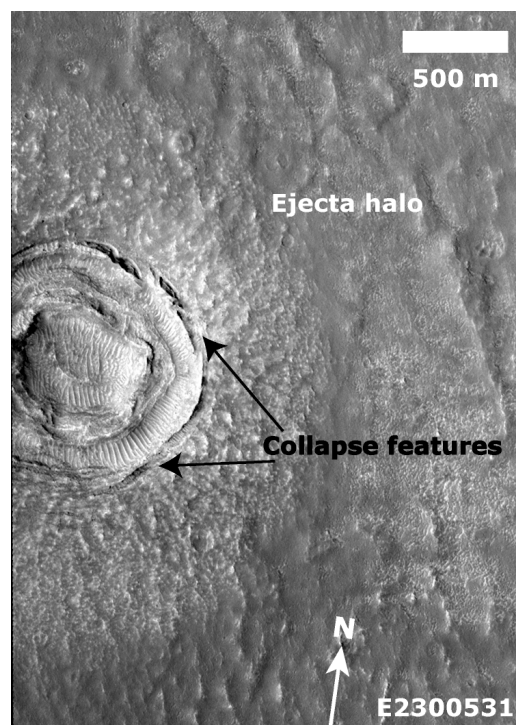


Figure 2. Portion of MOC image detailing morphology of Crater B. See Figure 1 for location.

Description of craters: The craters are ~1,200-1,800 m in diameter, although Crater D (Fig. 1) is ~2,600 m across. The crater morphology is dominated by a central depression surrounded by concentric fractures and faults (Fig. 2). The craters often have a double-ring center, characterized by an inner raised ring within the central depression (Fig. 2). Where MOLA profiles cross the craters, the craters do not have raised rims (Fig. 3) and may be as much as 70 m deep. MOC images show that two of the craters, B and D, have unequivocal evidence for some type of ejecta on the rim. The ejecta surrounding Crater D appears to have been more fluidized than the ejecta from Crater B. It is possible that the material ejected from Crater D may have had a slightly higher volatile content or been emplaced at a much lower angle to the substrate.

The available MOLA, THEMIS and MOC data were inspected for evidence consistent with either a formation resulting from collapse or formation by explosive activity within the flow deposit (which may be a mudflow), or a combination of the two processes. In this study, the classification of a “thermally distinct” crater is defined as a crater having a low-temperature interior surrounded by a high temperature halo relative to the surrounding surfaces in the nighttime IR data (Fig. 4).

The craters also have distinct thermal properties. Some craters are characterized by ejecta blankets that appear cooler than the surrounding material in the day IR and warmer than the surrounding material in the night IR (Fig. 4). In the nighttime IR, the innermost regions of the craters are generally 8-10 K cooler than the surrounding terrain, while the crater ejecta is ~5 K warmer than the underlying terrain. The cool daytime and warm nighttime ejecta on the rims of the craters is typical of a surface that is either blockier than the surroundings or more highly indurated than the surrounding material [5]. The low-temperature night IR signature of the central portion of the craters is characteristic of a dusty or fine-grained material, while the higher temperature of the outer halo is typically a rockier material [5]. In contrast, typical examples of impact craters in the region are characterized by ejecta that appear warm in the day IR and cool in the night IR.

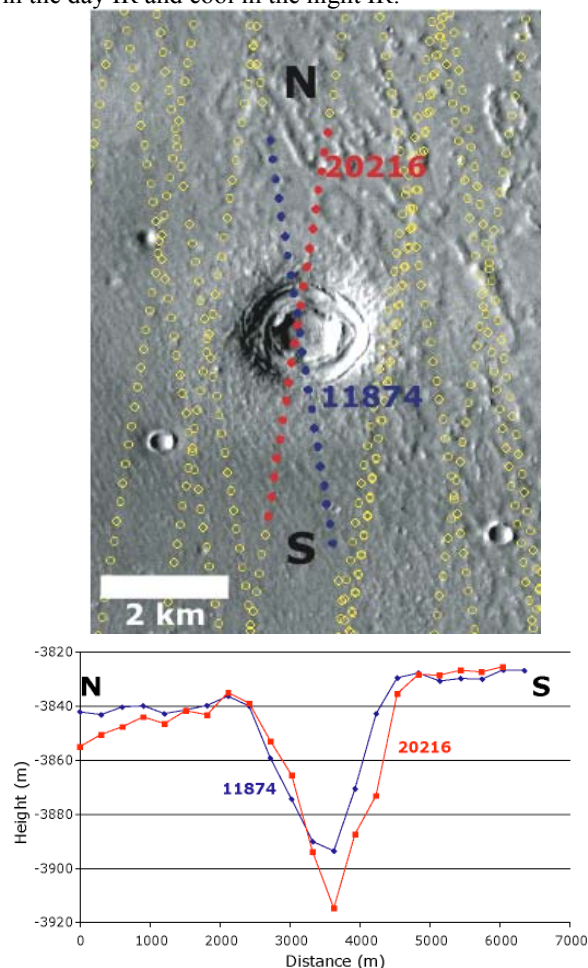


Figure 3a-b. MOLA topographic profiles of Crater B over portion of THEMIS VIS image V0263019. See Figure 1 for location.

Distribution of craters: The craters identified as thermally distinct craters based on the THEMIS night

IR data were mapped on a mosaic of Viking images (Fig. 2). Twelve craters were identified, all located in a region mapped as Apf (Amazonian fluted plains material) [6]. The Apf unit is characterized by smooth, level plains material having low-relief fluting and an intersecting pattern of linear hollows [6]. The Apf unit is interpreted as dune fields or a mudflow originating from the source of Hrad Vallis and Galaxias Fossae [6].

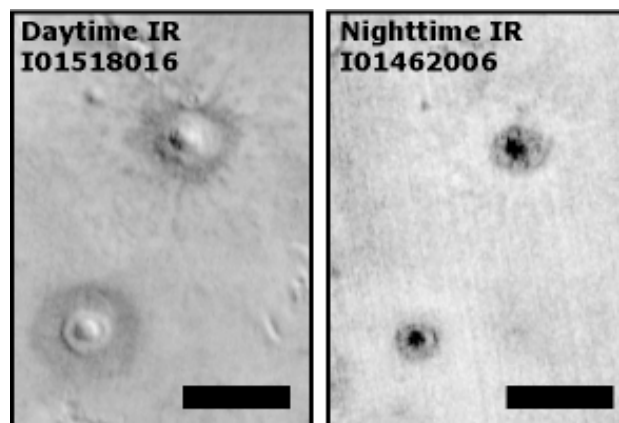


Figure 4. Day and night THEMIS IR images. 5 km scale bar. See Figure 1 for location.

Interpretations: The thermally distinct craters exhibit morphologies consistent with formation by explosion (ejecta surrounding the depression) and collapse of the surrounding material (fractures cutting some ejecta). A phreatic explosion within a mudflow would be expected to produce ejecta surrounding a central depression, although the exact volume of material ejected from the crater versus the volume of material that falls back into the crater is unknown. The observation that only the largest craters have ejecta that are visible in the available images may be consistent with the hypothesis that the larger craters are the result of a more energetic explosion that was more efficient at ejecting material out of the crater onto the surrounding terrain. The liberation of the locally concentrated volatiles may result in slumping of the newly formed crater walls in response to the free surface exposed within the crater.

Conclusions: The characteristics of the craters are consistent with a formation initiated by an explosive event followed by collapse of the region surrounding the depression. The origin of these explosions is being investigated.

References: [1] Christiansen E. H. (1989) *Geology*, 17, 203-206. [2] Wilson, L. and Mouginis-Mark P. J. (2003) *JGR*, 108, doi:10.1029/2003JE001927. [3] Mouginis-Mark P. J. et al. (1984) *Earth, Moon and Planets*, 30, 149-174. [4] Mouginis-Mark, P. J. (1985) *Icarus*, 64, 265-284. [5] Christensen, P. R. et al. (2003) *Science*, 300, 2056-2061. [6] De Hon, R. A. et al. (1999) *USGS Map I-2579*.